ELSEVIER

Catalysis Today 66 (2001) 487–494

CATALYSIS TODAY

www.elsevier.com/locate/cattod

Comparison of the efficiency of immobilized and suspended systems in photocatalytic degradation

M.F.J. Dijkstra*, A. Michorius, H. Buwalda, H.J. Panneman, J.G.M. Winkelman, A.A.C.M. Beenackers

Department of Chemical Engineering, University of Groningen, Nijenborgh 4, 9747 AG, Groningen, The Netherlands

Abstract

The photocatalytic degradation of formic acid in suspended and immobilized systems, with and without oxygen addition, are compared. In the immobilized system, oxygen addition to the reactor appeared to increase the efficiency, not only because oxygen acts as an efficient electron scavenger, but also due to increased mass transfer in this two-phase reactor. This immobilized system had an efficiency comparable to that of the suspended system. The addition of oxygen to the immobilized system appeared to increase the quantum yield with a factor 4, whereas the addition of oxygen to the suspended system hardly had any effect.

Keywords: Photocatalysis; Water purification; Quantum yield

1. Introduction

The purification of wastewater from toxic substances has become a major concern. Quality criteria for both surface water and drinking water tend to become more and more severe with time. In order to cope with these growing demands, new water purification methods are investigated [1,2]. Heterogeneous photocatalysis appears to be a promising novel technique. In this advanced oxidation process almost any organic contaminant can be completely degraded to carbon dioxide, water and mineral acids [3]. This complete destruction of the contaminants is a major advantage of heterogeneous photocatalysis, because no polluted phase remains after the purification as opposed to phase transfer methods (e.g. air stripping, adsorption on activated carbon) [4].

Advanced oxidation processes involve strongly oxidizing hydroxyl radicals, which degrade the pollutants. In heterogeneous photocatalysis, hydroxyl radicals are also assumed to be the reactive species [2,5]. The catalyst in this process is a semiconductor (mostly titanium dioxide) which is activated with near UV light. When a photon with an energy equal to or exceeding the band gap energy of the semiconductor ($h\upsilon \geq E_{gap}$) reaches the surface, an electron (e^-_{cb}) is promoted from the valence band to the conduction band. At the valence edge an electronic vacancy or hole (h^+_{vb}) is created. Both energy carriers can participate in various reactions: the holes and electrons can recombine and the energy will be lost as heat; they can get trapped in metastable surface states; and they can migrate to the surface of the semiconductor and participate in redox reactions with electron donors and electron acceptors adsorbed at the surface [2,6].

To prevent the electron–hole recombination, a suitable scavenger or surface defect state must be available to trap the electron or hole. Howe and Grätzel

* Corresponding author.
E-mail address: m.f.j.dijkstra@chem.rug.nl (M.F.J. Dijkstra).

0920-5861/01/$ – see front matter
PII: S0920-5861(01)00257-7

Nomenclature

a_{imm}	specific immobilized surface area (m^{-1})
a_{sus}	specific suspended surface area (m^{-1})
A_{cat}	external catalyst area (m^2)
C	concentration of formic acid ($g\,m^{-3}$)
C_{max}	saturation concentration of oxygen ($g\,m^{-3}$)
C_{TiO_2}	concentration catalyst ($g\,m^{-3}$)
C_0	initial concentration of formic acid ($g\,m^{-3}$)
d	hydraulic diameter (m)
d_p	diameter of the catalyst agglomerates (m)
I_0	amount of photons entering the reactor (Einstein s^{-1})
k_l	mass transfer coefficient ($m\,s^{-1}$)
k_r	Langmuir–Hinshelwood rate constant ($g\,m^{-3}\,s^{-1}$)
k_0	pseudo 0th order rate constant ($g\,m^{-3}\,s^{-1}$)
k_1	pseudo 1st order rate constant (s^{-1})
K_{ads}	Langmuir–Hinshelwood adsorption constant ($m^3\,g^{-1}$)
Re	Reynolds number (−)
t	reaction time (s)
T	temperature (K)
v	superficial velocity ($m\,s^{-1}$)
V_{reac}	volume of the reactor (m^3)
V_{tot}	total liquid volume in the recirculating batch system (m^3)
W_{cat}	amount of catalyst immobilized on tube ($g\,m^{-2}$)

Greek symbols

η	viscosity (Pa s)
ρ	density ($kg\,m^{-3}$)
ρ_{TiO_2}	density of titanium dioxide ($kg\,m^{-3}$)
Φ	quantum yield (−)

[7] showed that the conduction band electrons in an oxygen-free aqueous solution are trapped at the particle surface, possibly with the formation of Ti^{3+}. In the presence of molecular oxygen, the electrons are trapped by oxygen, forming the superoxide radical anion. The holes in the valence band migrate to the surface where they can react with water or hydroxide ions to produce hydroxyl radicals. These hydroxyl radicals are assumed to be the primary oxidizing species in the photocatalytic oxidation of organics, but also the positive holes can attack organic species at the surface [5].

In photocatalytic research, laboratory scale equipment has been used mostly. In our research group a project has started focusing on the development of a continuous photocatalytic reactor, which can be scaled up to industrial scale. Important parameters in the design of such a scalable photoreactor are: configuration of the catalyst, specific illuminated catalyst area, mass transfer characteristics, light efficiency, availability of oxidant and scaling possibilities.

The catalyst can be either immobilized or suspended in the reactor. So far, suspended systems have received most attention in literature. Although, the suspended system has the advantage of a larger surface area as compared to the immobilized system, the necessary separation of the nanometer catalyst particles is expensive and constitutes a major drawback in the commercialization of this system. The catalyst surface is only active if the catalyst particle is illuminated. To illuminate all the catalyst particles in the suspended system is difficult, because the particles further away from the light source are shielded from the radiation by those near the light source. Hence, the penetration depth of light into suspension is limited. In the immobilized system, it is possible to obtain a configuration in which all the catalyst is illuminated (e.g. a thin layer coated on a tube surrounding a tube light). A disadvantage of this system is that mass transfer limitation can easily occur [8,9]. The optimal reactor configuration has the highest possible illuminated specific catalyst area fixed on a support material which uses the light efficiently.

The objective of the present work is to compare the efficiency of the photocatalytic degradation of formic acid in both a slurry system and an immobilized system. Formic acid is chosen as model component because no intermediates are formed during its degradation. Parameters which will be taken into account are the specific surface area, the initial concentration of the pollutant, the concentration of the oxidant (dissolved molecular oxygen), the mass

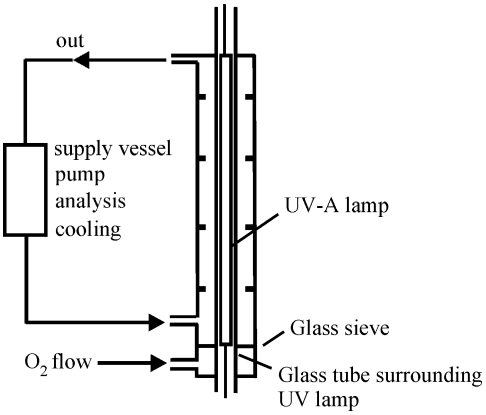

Fig. 1. Scheme of experimental set-up.

transfer characteristics and the quantum yield. From the results, conclusions for the development of an optimal reactor design will be drawn.

2. Experimental methods

2.1. Equipment

The experiments with suspended and the immobilized catalysts were performed in the same reactor to be able to compare the performances accurately. The reactor is a 124×10^{-6} m^3 double wall tubular reactor of borosilicate glass, see Fig. 1. The liquid was fed tangentially into the reactor and baffles were present in the reactor to reduce possible mass transfer limitations. The experiments were performed in a recirculating batch system consisting of a pump, cooling device, reactor vessel and a supply vessel. Cooling was provided by a Tamson 1000 thermostatic bath. In the inner tube a Philips TL29D15/09 (Cleo 15 W) UV-A lamp was placed. The total UV-A radiation was 1.8 W and the lamp had a wavelength spectrum of 300–410 nm with a maximum at 355 nm. The light intensity entering the reactor was determined by potassium ferrioxalate actinometry as described elsewhere [10].

In the immobilized system the catalyst was coated onto the outer wall of the inner tube by dipcoating (see below). Air was supplied through a glass mesh at the bottom of the reactor (Fig. 1), or through a sparger in the supply vessel. The total volume of the system was 650×10^{-6} m^3.

A Verder gear pump V540.05 was used for liquid circulation. In contrast, a Watson–Marlow 604U/R pump was used in the suspended system. Here, the total volume was 500×10^{-6} or 650×10^{-6} m^3. Air was supplied by a sparger present in the supply vessel.

2.2. Chemical substances

Degussa P-25 titanium dioxide was used as photocatalyst without further pretreatment. It has a BET surface of 55 m^2 g^{-1} and a particles size of 30 nm, which form agglomerates of 0.1–0.3 μm. Purified water (Millipore Milli-Q) was used to make the formic acid (reagent grade, Merck, 98–100%) solutions. Preliminary tests revealed that formic acid was not degraded by UV-A light alone. Only in the presence of both titanium dioxide and UV-A light, a rapid decrease in concentration was observed.

2.3. Analysis

Formic acid was analyzed off-line with capillary electrophoresis. A deactivated uncoated fused silica capillary with an internal diameter of 0.75 μm was used. The electrolytic solution was 4.6 mM chromate and 0.46 mM OFM-Anion-BT in Milli-Q water, where the pH was adjusted to 8 with sulfuric acid. Before use the electrolytic solution was vacuum filtrated over a 0.45 μm nylon filter for 10 min to remove air bubbles. Oxygen was analyzed on-line with an INGOLD oxygen electrode.

2.4. Catalyst immobilization

The catalyst was adhered onto the glass tube by dipcoating. The glass tube was thoroughly cleaned by ultrasonic rinsing with ethanol, dichloromethane, a mixture of $NH_3/H_2O_2/H_2O$ (1:1:5 v/v) and a mixture of HCl/H_2O (1:6 v/v). Between the different steps, the glass was thoroughly rinsed with Milli-Q water and afterwards dried for 1 h at 393 K. A 5% (w/w) suspension of titanium dioxide in water was prepared with Milli-Q water and ultrasonic mixing for 1 h. The glass tubes were dipped in the solution at a constant velocity of 1.3×10^{-3} m s^{-1} with a dipcoating apparatus as described elsewhere [11]. Between the dips the

layer was dried at room temperature for 10 min. The tubes with the immobilized catalyst were annealed by raising the temperature gradually with 3° per minute to avoid cracking of the layer, to a maximum temperature of 573 K at which it remained for 3 h. After this period the temperature was decreased with 5° per minute to room temperature. The total amount of catalyst on the tube was determined gravimetrically and varied from 0 to 3.6 g m^{-2}.

2.5. Experimental procedure

Prior to each experiment, the lamps were preheated for 30 min to obtain a constant light intensity. Before a tube with titanium dioxide was used for the first time, it was rinsed with Milli-Q water with the lamp turned on for 15 h to make sure that no pollutants were present on the catalyst surface. In the experiments with the suspended system, the titanium dioxide was ultrasonically suspended in Milli-Q water for 30 min just before the start of an experiment. Experiments with variable amounts of catalyst, various initial acid and oxygen concentrations and flows were performed. The temperature of the cooling water was 293 K and the Reynolds number, defined as $\rho v d/\eta$, in the system varied between 720 and 2400 corresponding to flows of $35 - 117 \times 10^{-6}$ m^3 s^{-1} (ρ is the density (kg m^{-3}), v the velocity in the reactor (m s^{-1}), d the hydraulic diameter (m) (defined as diameter of outer tube minus diameter of inner tube) and η the viscosity (Pa s)). The air flow in the immobilized system was 2.5×10^{-5} m^3 s^{-1}.

3. Results and discussion

3.1. Suspended system

With the suspended system it is important that all the catalyst reaches the illuminated zone in the reactor. Since, the penetration depth of the light in the fluid is small, the flow rate should be high enough to guarantee the necessary degree of mixing of the fluid in the reactor. Preliminary measurements with variable flow rates in the suspended system showed that the degradation of formic acid was independent of the flow rate, indicating that the catalyst could reach the illuminated zone in the reactor.

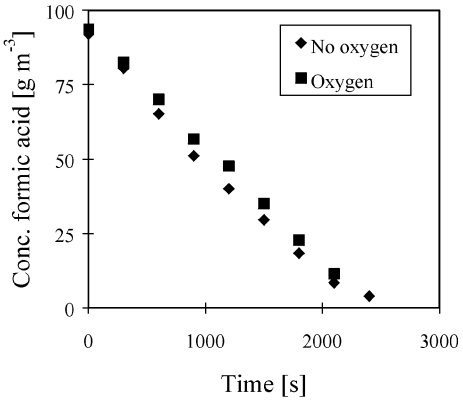

Fig. 2. The influence of oxygen addition on the degradation rate in the suspended catalyst system. $[TiO_2] = 500$ g m^{-3}, $V_{tot} = 650 \times 10^{-6}$ m^3, $Re = 1440$, $T = 293$ K.

The addition of oxygen had hardly any effect in the suspended system, see Fig. 2. The concentration of oxygen decreased to 60% of the maximum saturated concentration ($C_{max} = 9$ g m^{-3}) in case of no oxygen addition whereas the concentration decreased 2% with oxygen added to the system. From these results it can be concluded that oxygen is not deficient at the surface. Extra addition of oxygen does not increase the reaction rate by decreasing the recombination rate of the electrons and holes in the semiconductor. A possible explanation for the slight decrease in activity is that the catalyst is less efficiently illuminated due to bubbles in the suspension.

3.2. Modeling of the suspended system

In photocatalysis the degradation of pollutants is often described with the Langmuir–Hinshelwood kinetics [5]. For the recirculating batch system the mass balance of formic acid can then be written as

$$-\frac{dC}{dt} = \frac{k_r K_{ads} C}{1 + K_{ads} C} \frac{V_{reac}}{V_{tot}} \quad (1)$$

where C is the concentration of formic acid (g m^{-3}), t the reaction time (s), k_r the reaction rate constant (g m^{-3} s^{-1}), K_{ads} the Langmuir–Hinshelwood adsorption constant (m^3 g^{-1}), V_{reac} the volume of the reactor (m^3) and V_{tot} the total liquid volume in the recirculating batch system (m^3). Two asymptotic situations can

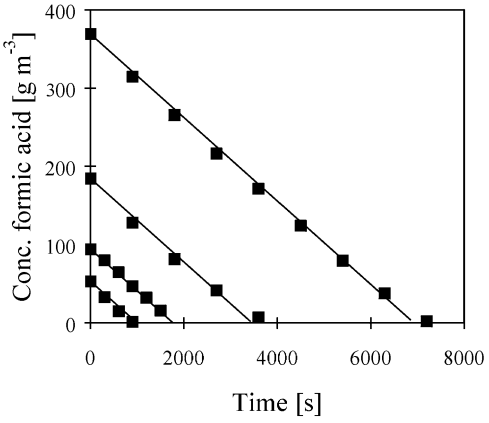

Fig. 3. The degradation of formic acid in the suspended catalyst system for various initial concentrations. Lines: pseudo 0th order model. $[TiO_2] = 250\,g\,m^{-3}$, $V_{tot} = 500 \times 10^{-6}\,m^3$, $Re = 1030$, $T = 293\,K$, no addition of oxygen.

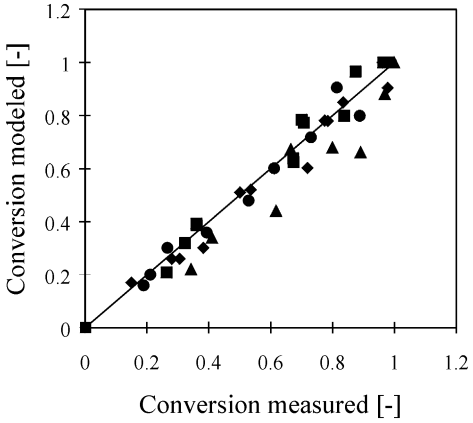

Fig. 4. Parity plot of the degradation in the suspended catalyst system, modeled with the pseudo 0th order model. Concentrations of TiO_2: (◆) $250\,g\,m^{-3}$, (■) $500\,g\,m^{-3}$, (●) $1000\,g\,m^{-3}$, (▲) $2000\,g\,m^{-3}$. Initial concentrations formic acid range: 50–$400\,g\,m^{-3}$.

be identified:

$$-\frac{dC}{dt} = k_r K_{ads} C \frac{V_{reac}}{V_{tot}} = k_1 C \frac{V_{reac}}{V_{tot}} \quad \text{for } 1 \gg K_{ads}C \text{ (pseudo 1st order)} \tag{2}$$

$$-\frac{dC}{dt} = k_r \frac{V_{reac}}{V_{tot}} = k_0 \frac{V_{reac}}{V_{tot}} \quad \text{for } 1 \ll K_{ads}C \text{ (pseudo 0th order)} \tag{3}$$

The degradation of formic acid was measured for various suspended catalyst concentrations (500–$2000\,g\,m^{-3}$). The degradation rate in the suspended system appeared to be successfully described by the pseudo 0th order model over a large concentration range, see Fig. 3. Slight deviation from the model for low concentration levels were observed which can be expected since then $K_{ads}C$ is probably no longer much larger than 1. The parity plot shown in Fig. 4 illustrates the ability of the pseudo 0th order model to describe the data obtained with the various catalyst concentrations applied.

The reaction rate constant shows a small increase with increasing catalyst loading from 0.5 to $2 \times 10^3\,g\,m^{-3}$, and seems to reach the maximum value for $2 \times 10^3\,g\,m^{-3}$ as has also been found by Aguado et al. [12], see Fig. 5.

3.3. Immobilized system

Immobilized systems often suffer from mass transfer limitation [8,9]. From experiments with variable flow rates, it was observed that the degradation rate of formic acid both with and without oxygen addition increased with increasing flow rate, indicating the presence of mass transfer limitation in our system as well, see Fig. 6. The shape of the curves shows that in this system the experiments cannot be described with the pseudo 0th order model. Due to the mass transfer limitation the surface concentration will be much lower,

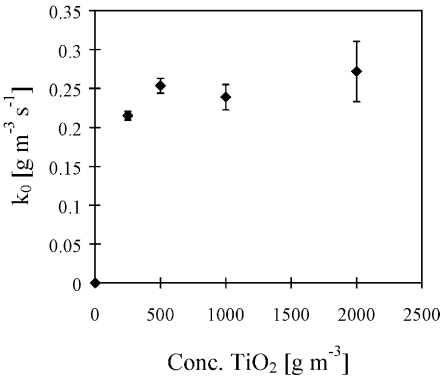

Fig. 5. Pseudo 0th order reaction rate constants with 95% confidence intervals.

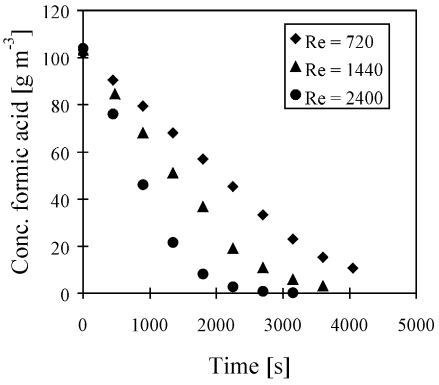

Fig. 6. The influence of the water flow rate on the degradation rate in the immobilized catalyst system with indirect oxygen addition in the reactor (one-phase in reactor). $W_{cat} = 3.6\,g\,m^{-2}$, $V_{tot} = 650 \times 10^{-6}\,m^3$, $T = 293\,K$.

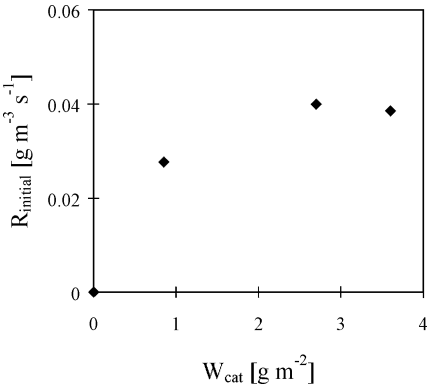

Fig. 8. The influence of the amount of catalyst on the initial degradation rate in the immobilized catalyst system, one-phase in reactor. $C_0 = 100\,g\,m^{-3}$, $V_{tot} = 650 \times 10^{-6}\,m^3$, $Re = 1440$, $T = 293\,K$.

causing the value of $K_{ads}C$ to be no longer much larger than 1. Therefore, the Langmuir–Hinshelwood kinetic model will describe these measurements as has also been found by Matthews [13] for the degradation of formic acid in an immobilized system.

Oxygen has a positive effect on the degradation rate in the immobilized catalyst system (Fig. 7). Oxygen acts as an electron scavenger, thus decreasing the recombination rate in the semiconductor [14]. The degradation rate in the system with oxygen bubbling through the reactor via a glass sieve (two-phases in reactor) is faster relative to that in the system with oxygen addition through a sparger in the supply vessel (one-phase in the reactor), see Fig. 7. Since the oxygen concentration remained the same during the experiments this difference appears to be caused by an increase of the mass transfer rate in the two-phase system. The mass transfer coefficient, k_l, is increased due to higher turbulence caused by the two-phase flow along the catalyst surface.

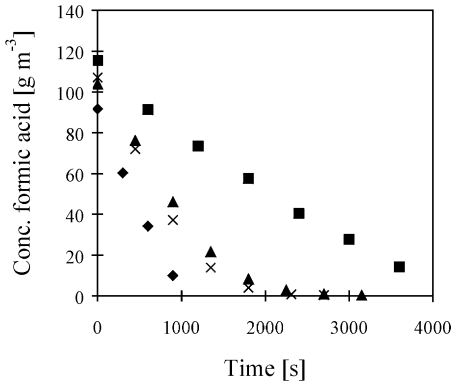

Fig. 7. The performance of the different systems: (◆) suspended catalyst system: $[TiO_2] = 2000\,g\,m^{-3}$, $V_{tot} = 500 \times 10^{-6}\,m^3$, $Re = 1030$, $T = 293\,K$, no addition of oxygen. (×) Immobilized system, addition of oxygen, two-phases in reactor: $W_{cat} = 3.6\,g\,m^{-2}$, $V_{tot} = 650 \times 10^{-6}\,m^3$, $Re = 2400$, $T = 293\,K$. (▲) Immobilized catalyst system, addition of oxygen, one-phase in reactor: $W_{cat} = 3.6\,g\,m^{-2}$, $V_{tot} = 650 \times 10^{-6}\,m^3$, $Re = 2400$, $T = 293\,K$. (■) Immobilized catalyst system, no addition of oxygen: $W_{cat} = 2.74\,g\,m^{-2}$, $V_{tot} = 285 \times 10^{-6}\,m^3$, $Re = 1030$, $T = 293\,K$.

With increasing amounts of catalyst coated on the tube the initial reaction rate increases until a maximum value is reached, see Fig. 8. This can be explained by an increased amount of light absorbed by the catalyst layer with an increasing layer thickness, until all the light falling on the catalyst will be absorbed and the maximum activity is reached. Also, mass transfer phenomena will influence the dependence of the reaction rate on the amount of catalyst, since mass transfer limitations will be more severe for higher reaction rates.

3.4. Suspended versus immobilized

For optimal comparison, the quantum yield, Φ, has been determined for the experiments depicted in Fig. 7. The quantum yield used here is defined as [2]

Table 1
Quantum yields of different systems[a]

	Slurry 2×10^3 g m^{-3}	Immobilized without O_2 addition	Immobilized O_2 addition one-phase in reactor	Immobilized O_2 addition two-phases in reactor
Specific area (m^2 m^{-3})[b]	10300	177[c]	177[c]	177[c]
Quantum yield (–)	0.28	0.063	0.22	0.28

[a] Quantum yields of experiments depicted in Fig. 7.
[b] $a_{sus} = 6C_{TiO_2}/\rho_{TiO_2}d_p$ with C_{TiO_2} is concentration catalyst (g m^{-3}), ρ_{TiO_2} is the density of titanium dioxide (g m^{-3}) and d_p is the diameter of the catalyst agglomerates (m). $a_{imm} = A_{cat}/V_{reac}$ with A_{cat} is the external catalyst area (m^2) [11].
[c] This value is actually higher, since the layer is porous.

$$\Phi = \frac{(dC_0/dt)V_{tot}}{I_0} \quad (4)$$

where dC_0/dt is the initial degradation rate (mol m^{-3} s^{-1}) and I_0 the amount of photons entering the reactor (Einstein s^{-1}). I_0 is equal for all three systems, because the same reactor and lamp were used. The value for I_0 was determined with actinometry as 4×10^{-6} Einstein s^{-1}.

In the two-phase system Φ is four times as high as that in the immobilized system without oxygen addition, see Table 1. In the suspended system Φ is comparable with that in the two-phase system, which is remarkable since the specific area is much larger in the suspended system. Due to the difference in kinetics (pseudo 0th order in suspended system versus Langmuir–Hinshelwood kinetics in immobilized system), the quantum yield in the immobilized system will decrease with initial concentration (dC_0/dt decreases), whereas in the suspended system it remains constant. The values for the quantum yield are comparable to values found for the degradation of formic acid by Sczechowski et al. [15].

Since, the quantum yield of the two-phase immobilized system is comparable to that of the suspended system and a costly separation step is necessary in the suspended system, an optimal reactor design for photocatalytic water purification will be an immobilized system optimized with respect to catalyst layer thickness, light intensity, specific area and mass transfer.

4. Conclusions

Formic acid can be easily degraded with heterogeneous photocatalysis. The degradation experiments in the suspended catalyst system can be very well modeled with the pseudo 0th order model. The activity of the suspended system reaches a maximum for 2×10^3 g m^{-3}. The addition of oxygen hardly affects the activity of the suspended system. The degradation experiments in the immobilized system show that mass transfer limitation occurs. Comparing the immobilized systems with and without oxygen addition, the system in which oxygen is introduced through a glass sieve in the bottom of the reactor appears to be more efficient, not only because oxygen acts as an efficient electron scavenger, but also due to increased mass transfer in this two-phase reactor. This immobilized system has a quantum yield which is comparable to that of the suspended system. Since the suspended system has the disadvantage of an expensive downstream separation step, it seems attractive to focus on the development of two-phase immobilized systems with maximum immobilized surface area per unit reactor volume and optimal light intensity and catalyst layer thickness.

Acknowledgements

This work was supported by the Netherlands Foundation for Chemical Research (SON) with financial aid from the Netherlands Technology Foundation. We like to thank Philips for their generous supply of UV lamps.

References

[1] O. Legrini, E. Oliveros, A.M. Braun, Photochemical processes for water treatment, Chem. Rev. 93 (1993) 671–698.
[2] M.R. Hoffmann, S.T. Martin, W. Choi, D.W. Bahnemann, Environmental applications of semiconductor photocatalysis, Chem. Rev. 95 (1995) 69–96.

[3] M.M. Halmann, Photodegradation of Water Pollutants, CRC Press, Boca Raton, 1996.
[4] D.F. Ollis, C. Turchi, Heterogeneous photocatalysis for water purification: contaminant mineralization kinetics and elementary reactor analysis, Environ. Prog. 9 (4) (1990) 229–234.
[5] C.S. Turchi, D.F. Ollis, Photocatalytic degradation of organic water contaminants: mechanisms involving hydroxyl radical attack, J. Catal. 122 (1990) 178–192.
[6] M. Schiavello, A. Sclafani, Thermodynamic and kinetic aspects in photocatalysis, in: E. Pelizzetti, N. Serpone (Eds.), Photocatalysis, Fundamentals and Applications, 1989, pp. 159–173.
[7] R.F. Howe, M. Grätzel, EPR observation of trapped electrons in colloidal TiO_2, J. Phys. Chem. 89 (1985) 4495–4499.
[8] D.F. Ollis, E. Pelizzetti, N. Serpone, Photocatalyzed destruction of water contaminants, Environ. Sci. Technol. 25 (9) (1991) 1522–1529.
[9] A.K. Ray, A.A.C.M. Beenackers, Novel swirl-flow reactor for kinetic studies of semiconductor photocatalysis, AIChE J. 43 (10) (1997) 2571–2578.
[10] S.L. Murov, Handbook of Photochemistry, Dekker, New York, 1973, pp. 119–123.
[11] A.K. Ray, A.A.C.M. Beenackers, Novel photocatalytic reactor for water purification, AIChE J. 44 (2) (1998) 477–483.
[12] M.A. Aguado, S. Cervera-March, J. Giménez, Continuous photocatalytic treatment of mercury(II) on titania powders. Kinetics and catalyst activity, Chem. Eng. Sci. 50 (10) (1995) 1561–1569.
[13] R.W. Matthews, Photocatalytic oxidation of organic contaminants in water: an aid to environmental preservation, Pure Appl. Chem. 64 (9) (1992) 1285–1290.
[14] A. Mills, S. Le Hunte, An overview of semiconductor photocatalysis, J. Photochem. Photobiol. A 108 (1997) 1–35.
[15] J.G. Sczechowski, C.A. Koval, R. D Noble, A Taylor vortex reactor for heterogeneous photocatalysis, Chem. Eng. Sci. 50 (20) (1995) 3163–3173.